Journal of Materials Chemistry B

Accepted Manuscript

ROYAL SOCIETY OF CHEMISTRY

www.rsc.org/materialsB

Synergistic mediation of tumor signaling pathways in hepatocellular carcinoma therapy via dual-drug-loaded pH responsive electrospun fibrous scaffolds

Ziming Yuan[a,c 1], Xin Zhao[a,1], Jingwen Zhao[a], Guoqing Pan[a,b], Wangwang Qiu[c], Xiaohu Wang[c], Yueqi Zhu[c], Qi Zheng[c,*], Wenguo Cui[a,b*]

[a] Orthopedic Institute, Soochow University, 708 Renmin Rd, Suzhou, Jiangsu, 215006, P.R. China.

[b] Department of Orthopedics, The First Affiliated Hospital of Soochow University, 188 Shizi St, Suzhou, Jiangsu, 215006, P.R. China

[c] Department of General Surgery, Shanghai Sixth People's Hospital Affiliated to Shanghai Jiao Tong University, School of Medicine, 600 Yishan Road, Shanghai, 200233, P.R. China.

[1] These authors contributed equally to this work.

[*] Corresponding author: Wenguo Cui, *E-mail:* wgcui80@hotmail.com; Tel. (Fax): (+86) 512-6778-1420.

[*] Corresponding author: Qi Zheng, *E-mail:*zhengqi1957@aliyun.com; Tel: (+86) 21-64369181; Fax: (+86)21-64701361.

Abstract

With the understanding of tumorigenesis, the tumor-infiltrating inflammatory cells, which could contribute to the carcinogenesis, have greatly drawn public attentions. We hypothesized that controlling inflammation in the initial stage combined with anti-tumor activity for a relatively long term could prevent the tumor recurrence. Here, we designed a novel electrospun composite poly (L-lactide) (PLLA) fibrous scaffold, which contained sodium bicarbonate (SB) and doxorubicin (DOX) inside mesoporous silica particles (MSNs) to achieve long-term pH-sensitive DOX release, and ibuprofen (IBU) outside MSNs to achieve initial short-term release. This construct was found to have an initial burst release of IBU at the early stage, and sustained release of DOX at a relatively later stage. *In vivo* results showed that when the fibrous scaffold was implanted in a liver-tumor-bearing nude mouse, the mouse life span has been prolonged to 1.5 times higher than that implanted with scaffolds with no IBU or SB. Moreover, the residual tumor treated with PLLA-(MSN/DOX-SB)-IBU fibers demonstrated considerable signs of apoptosis and large areas of necrosis over a 10 week examined period. Combined the *in vitro* and *in vivo* experiments, the results have suggested that this dual-drug delivery system could effectively inhibit the inflammation at the initial stage and prevent the tumor recurrence for a relatively long term and may find application as local implantable scaffolds to treat a tissue defect after tumor resection.

Keywords: Hepatocellular carcinoma; Residual tumor; Inflammation; Dual-drug; Drug-delivery.

1. Introduction

Liver cancer is the second leading cause of cancer death, which resulted in 746,000 deaths in 2012.[1] Among primary liver cancers, hepatocellular carcinoma (HCC) accounts for 90%.[1] Current therapies including resection, transplantation, ablation and chemoembolization have improved the survival of patients diagnosed at early HCC stages, among which, surgical resection is the most promising strategy.[2, 3] However, the procedure suffers from recurrence rate of 20-64% in the first year and 57-81% at 3 years after curative resection because of the presence of tumor or undetected residual intrahepatic defects.[4, 5] Therefore, the prevention of recurrence for a relatively long term is particularly important to improve the success rate of the surgery.

Tumor recurrence is mostly detected in remnant liver and a number of local treatment strategies have been developed to minimize the probability of post-surgical local recurrence.[6] Some previously studies have shown encouraging results with the use of postoperatively adjuvant transarterial chemotherapy (ATAC).[7] However, in more recent times, a randomized controlled trial showed that the patients treated with either transarterial or systemic adjuvant chemotherapy after HCC resection, were associated with more frequent extrahepatic recurrences.[7] Hence, searching new directions of therapy and/or developing new drug combination therapy, are still the emphasis in the field of HCC treatment.

Tumor microenvironment is a dynamic system and could be largely orchestrated by inflammatory cells.[8] During tumorigenesis, tumor-infiltrating inflammatory cells can produce variety of cytokines, such as interleukin-6 (IL-6) and tumor necrosis factor (TNF)-α, which contribute to carcinogenesis by persuading the survival, proliferation, differentiation and metastasis of tumor cells.[9] On the other hand, surgical trauma itself can cause a host inflammatory reaction, involving IL-6, TNF-α and many other cytokines,[10] and the surgery-induced hypoxia unfavorably affects the likelihood of tumor recurrence by inducing angiogenesis associated with residual tumor growth and metastasis.[11] Because inflammation is a potential contributor to

tumor recurrence, and rapid control of inflammation, improving the tumor microenvironment is the top priority after operation. Only the inflammation was controlled, the antitumor drugs can play a better role. So the quick release of anti-inflammatory drugs were needed. Furthermore, diseased tissue results in the hypoxia and lactic acid accumulation so that pH of tumor is lower than normal tissues.[12] Hence, cancer treatment can utilize acid-responsive systems to trigger drug release in tumor environment. Therefore, it is expected that integration of anti-inflammation activity in the cancer therapy which can respond to tumor environment may be beneficial to increase its therapeutic efficacy. If such hypothesis is proven to be true, the findings will help elucidate the mechanism underneath the inflammation and tumor recurrence which has not been clearly revealed so far.

Electrospun fibrous scaffolds are promising candidates as tissue engineering scaffolds as well as drug delivery devices.[13, 14] Nevertheless, because of their large surface area to volume ratio, it is difficult to achieve long-term drug release using the naked electrospun fibers.[15] Previously, we incorporated the drug-loaded mesoporous silica nanoparticles (MSNs) into electrospun poly (L-lactide) (PLLA) fibers and achieved the long-term drug delivery of more than three months via increasing the drug diffusion routes.[16] Therefore, it is conceived that when this system is used for anti-tumor drug delivery, it could suppress the tumor growth for a long period. However, the development of electrospun fiber-based HCC therapy has been hampered by two major obstacles: (i) temporally controlled dual-drug delivery electrospun fibers to control inflammation at the early stage and to release anti-tumor drug for the long-term, and (ii) environment responsive drug delivery based on reduced pH of tumor environment. In present study, we addressed these challenges through environment responsive dual-drug electrospun fibers which can sequentially release anti-inflammation and anti-tumor drugs. This regimen may also mediate tumor signaling pathways in HCC therapy.

In order to achieve anti-inflammation at the initial stage and anti-tumor for a relatively long term in one system, here, we designed a multifunctional electrospun

fiber consisting of sodium bicarbonate (SB, $NaHCO_3$)-loaded MSNs which could induce drug release in acidic environment because of quick reaction of $NaHCO_3$ and acid. Once the fibers were transported into an acidic environment, the protons (H^+) reacted with the $NaHCO_3$ contained in the fibers, and CO_2 gas was generated which created channels inside the fiber. Anti-inflammatory ibuprofen (IBU) was incorporated outside the MSNs, which would be burst released in the early stage, and the other drug, anti-tumor doxorubicin (DOX), was loaded inside MSNs with $NaHCO_3$ and could be released in respond to reduced pH for a long term. As it was reported that the adjuvant chemotherapy for HCC should be started soon after resection,[17] we implanted this multifunctional drug delivery system in the remnant liver immediately after the hepatectomy. *In vitro*, the structure and release profile of the electrospun fibers were investigated. *In vivo*, the therapeutic effect of this material was investigated and the anti-tumor mechanism of this material was further studied. This strategy may be a promising approach of localized bioresponsive long-term dual drug release which may be translatable to human tumors for prevention of mammary tumor progression. In addition, the results may provide some hints of the mechanism of inflammation and tumorigenesis.

2. Materials and methods

2.1. Materials

PLLA (Mw = 100 kDa, PDI = 1.6), 3-(4,5-dimethyl-thiazol-2-yl)-2,5-diphenyltetrazolium bromide (MTT) and dimethylsulfoxide (DMSO) were purchased from Sigma. Dichloromethane (DCM), SB ($NaHCO_3$), N,N-dimethylformamide (DMF), tetraethylorthosilicate (TEOS) (98% pure), 3-aminopropyltriethoxysilane (APTES) (99% pure) were all of analytical reagent grade and were from the Sinopharm Chemical Reagent Co., Ltd. Dulbecco's modified Eagle's medium (DMEM), fetal bovine serum (FBS), and phosphate buffered saline (PBS) were obtained from Gibco. Ammonia-catalyzed hydrolysis was performed on TEOS to produce MSNs.[16] M-PER mammalian protein extraction

reagent for western blot was from Thermo Scientific. Trizol reagent kit and M-MLV reverse transcriptase were from Invitrogen. Antibodies against caspase-3, IL-6, STAT3, NF-κB and glyceraldehyde-3-phosphate dehydrogenase (GAPDH) were from Abcam. The secondary horseradish peroxidase (HRP)-linked antibodies were obtained from Boster (Wuhan, China). All other chemicals and solvents were of reagent grade or better and were purchased from the Guo Yao Reagents Company (Shanghai, China), unless otherwise indicated.

2.2. DOX-loaded mesoporous silica nanoparticles

MSNs were synthesized using a modified Stöber method as described previously.[18] The particle size distribution of the synthesized MSNs was analyzed using particle size analyzer (Nano ZS, Malvern Instruments Ltd).

200 mg as-prepared MSNs was added into 20 ml of 60% methanol, either fully or 25% saturated with DOX, labelled as MSN/DOX. The mixture was stirred for 12 h at 37°C to allow DOX encapsulation into MSNs. The mixture was then centrifuged to collect the particles and washed twice using 60% methanol. The pellet after centrifuge was then collected and air-dried for further studies. Then, MSN/DOX pellet was added into 0.12 ml of $NaHCO_3$ saturated water solution (96 mg/ml) slowly with vigorous stirring for 24 h with a magnetic stirrer. MSN/DOX-SB was collected and air-dried, and the supernatant was collected for further studies. The acetone was added into the supernatant at a ratio of 5/2 (v/v), and the residual $NaHCO_3$ in the supernatant was precipitated. After centrifuge, the amount of absorbed $NaHCO_3$ in MSN-DOX was calculated via weighing the MSNs before and after $NaHCO_3$ incorporation. The UV-vis spectroscopy was used to determine the amount of DOX in all the supernatants to obtain the amount of drugs loaded inside MSNs.

2.3. Synthesis of electrospun fibrous scaffold

Fabrication of the electrospun PLLA fibers was described in our previous report.[16] Briefly, PLLA (1.0 g) was first completely dissolved in DCM (4 g) and DMF (2 g). To prepare the PLLA-DOX electrospun solution, 1.0 g PLLA with 5.0 mg DOX was first dissolved in 4.5 g of solvent mixture composed of DCM, HFIP and

EtOH (5:2:2, v/v/v). For the PLLA-MSN/DOX and PLLA-(MSN/DOX-SB) electrospun fibers, the as-prepared MSN/DOX or MSN/DOX-SB (200 mg MSN) was then added into the PLLA solution (1.0 g PLLA, 4.0 g DCM and 2.0 g DMF) and sonicated until fully dispersed. For the PLLA-(MSN/DOX-SB)-IBU electrospun fibers, 50 mg IBU was firstly dissolved into mixture solvent of DCM (4.0 g) and DMF (2.0 g), and then 1.0 g PLLA with MSN/DOX-SB (200mg MSN) was added into the IBU solution until PLLA fully dissolved.

Environmental scanning electron microscopy (ESEM, FEI, QUANTA250, the Netherlands) was used to characterize the morphology and dimensions of synthesized MSNs and fibrous scaffolds. Transmission electron microscopy (TEM, JEM-2100F, Japan) was used to investigate the MSN structure and its encapsulation inside the PLLA fibers.

2.4. In vitro drug loading study

200 mg of dried samples were immersed in 15 ml phosphate-buffered saline (PBS) and the solutions were placed under 100 rpm shaking at 37°C for 120 days. At pre-determined time points, 1 ml PBS was replaced with 1 ml fresh PBS and UV-vis spectroscopy (absorbance at 480 nm for DOX or 264 nm for IBU) was used to analyze the amount of released drugs in the collected PBS via comparison with standard curves of DOX [19] or IBU [16]. The percentage of drug release was calculated based on the amount of initially incorporated drug. This study was performed in triplicate for each formulation.

2.5. Cell line and culture

The human hepatocellular carcinoma cell line (HuH-7) was purchased from the Cellular Biology Institute of the Chinese Academy of Sciences (Shanghai, China). Cells were cultured in DMEM supplemented with 1% penicillin/streptomycin, and 10% FBS, and kept at 37°C in an atmosphere of 5% CO_2 and humidified air. Media were changed every 2 days. When cells reached about 80% confluence, they were subcultured by trypsinization with a trypsin (0.25%)-EDTA (0.03%) solution.

2.6. Animals

Balb/c mice of about 5-6 week old with an average body weight of 20-25 g were obtained from the Animal Breeding Center, Shanghai Sixth People's Hospital Affiliated to Shanghai Jiao Tong University, School of Medicine, China. The animals were housed in standard size polycarbonate cages (5/cage) fed with standard pellet diet and water freely, at the temperature about 26 ± 1°C and 12 h light/dark cycles.

2.7. In vivo tumor models

All the animal experiments were authorized according to the Guidance Suggestions for the Care and Use of Laboratory Animals (issued by the Ministry of Science and Technology of the People's Republic of China), and was approved by the Ethics Committee of the Sixth People's Hospital Affiliated to Shanghai Jiao Tong University. HuH-7 cells were used for tumor inoculation when they reached 80% confluence and tumors were established by subcutaneously injecting 2×10^6 cells /0.1ml/site into the front flank of the mice. The size of the developed tumors was monitored every other day and the animals were subjected to *in vivo* experiments when the tumor size reached about 100 mm^3 (typically 2 weeks after inoculation). Then a part of tumor was removed and different scaffolds were implanted into the remnant tumor. The day to implant scaffolds was assigned as day '0'. On day 1, the animals were randomly divided into six groups (each group n = 15). Control mice underwent partial tumor excision and were left untreated. The fiber scaffold implanted in every mouse was sectioned as 0.5×1.0 cm^2, weighted 5 mg, and the content of DOX and IBU administered to each animal were about 25 μg and 250 μg, respectively. The experimental groups were noted as PLLA, PLLA-DOX, PLLA-MSN/DOX, PLLA-(MSN/DOX-SB) and PLLA-(MSN/DOX-SB)-IBU. The animals were observed three times a week to obtain the information regarding tumor size, body weight, survival time and number of long-term survivors, and euthanized on the third day, the second, sixth and tenth week (n=5) post scaffold implantation. Then samples of the subcutaneously localized tumor remnant were harvested and bisected, one half fixed in 10% formalin for the histological and immunochemical analysis, and the other half deposited in liquid nitrogen for the following PCR and Western blot

analysis.

2.8. The percentage increase in life span

The effect of different scaffolds on percentage increase in life span was calculated according to the mortality of the tumor-bearing nude mice. To determine the mean survival time (MST) and percentage increased life span (% ILS), the animals were allowed to progress to a natural death. The % ILS equals to MST of treated group / MST of control group × 100.[20]

2.9. Measurement of C-reactive protein

Inflammation causes macrophages and adipocytes to multiply and secrete factors that trigger the liver to synthesize C-reactive protein (CRP) and acute-phase protein found in blood plasma.[21] In this study, venous blood samples were collected immediately before and after the operation. The serum samples for plasma protein analysis were stored frozen at -70°C. A sandwich enzyme-linked immunesorbent assay (ELISA) was employed for the measurement of C-reactive protein (CRP) according to the manufacturer's recommendations (RD). Briefly, the 96-well microtiter plates were coated with purified nude mouse CRP antibody. The CRP of samples was then added to each well, followed by addition of horseradish peroxidase (HRP) labeled CRP antibody. After complete washing, this antibody-antigen-enzyme-antibody complex reacted with the substrate solution 3, 3', 5, 5'- tetramethyl benzidine (TMB). The plates were then read at the wavelength of 450 nm using a Labsystems Multiskan MS 352 ELISA plate reader (Labsystems, Finland), and the CRP concentrations in the samples were determined by comparing the OD of the samples with the standard curve.

2.10. Histological analysis of the residual tumor tissues

At 37°C, the tumors collected from sacrificed mice were immersed in 10% formalin for 24 h. After being dehydrated in ethanol and cleared in xylene, the tumor samples were then embedded in paraffin and sliced into 5 μm sections. Finally, samples were stained in hematoxylin and eosin (H&E) for histological analysis regarding inflammatory reaction, necrosis, mitotic figures, etc.

2.11. The content of lactic acid of neoplastic tissues

As lactic acid accumulation occurs during tumor progression, the content of lactic acid is used to indicate the status of tumor development [22]. Lactic acid was determined by p-Hydroxybiphenol Colorimetry. Briefly, frozen tissues were ground, lysed using cell lysis buffer and centrifuged to obtain the supernatant. The supernatant containing lactic acid would then react with concentrated sulfuric acid with the catalysis of copper ions, generating acetaldehyde. Then, the resultant acetaldehyde reacted with the p-hydroxybiphenol and produced purple substances, which has characteristic absorption at the wavelength of 565 nm.

2.12. Measurement of caspase-3 activity

Caspase 3 is an apoptosis-related cysteine peptidase. Sequential activation of caspases plays a crucial role in the execution-phase of cell apoptosis.[23] Caspase 3 activity can thus be used to indicate the apoptotic activity of cells. To quantify the caspase-3 activity of the fresh tissues, the corresponding assay kit was used (KeyGEN BioTECH, Nanjing, China). Briefly, the whole protein fraction was extracted with the lysis buffer and the supernatant was kept. 1~2 μl of supernatant was used to determine the protein concentrations with the BCA method. Then, with a final volume of 50 μl, each reaction container was placed on ice followed by adding 50 μl of 2× reaction buffer. After that, 5 μl of caspase-3 substrate (Ac-DEVD-pNA, 1 mM) was added into the above system which was then incubated without light at 37°C for 4 h. Finally, the absorbance at 405 nm was measured by an automated spectrophotometer (Tecan, Switzerland), and the activation extent of caspase-3 was calculated with the formula: caspase-3 activation extent = $OD_{experiment}$ / $OD_{blank\ control}$. The mixture of lysis buffer and 2× reaction buffer acted as the blank control.

To examine the distribution of caspase-3 in fresh tissues, the immunohistochemical staining was performed. Firstly, the sections were hydrated, and the antigen retrieval was performed by incubating the sections in 10 mM sodium citrate buffer (pH 6.0) at 80°C for 10 min. After the addition of 1% hydrogen peroxide to block endogenous peroxidases, sections were further blocked by adding 1.5%

normal serum. Following overnight incubation with caspase-3 primary antibodies (1:400; Abcam) at 4°C under humid condition, sections were further incubated with horseradish peroxidase (HRP)-conjugated secondary antibodies (1:1000) for 30 min at room temperature. 3,3'-diaminobenzidine tetrahydrochloride (DAB) reagent was used to observe immune reactions. The negative control was one without primary antibodies. Hematoxylin was used for counter-staining prior to imaging using a light microscope (Eclipse TS100, Nikon, Japan).

2.13. Measurement of Bax: Bcl-2 ratio

By following manufacturer's protocol, Trizol (Invitrogen) was employed to extract total RNA from tumor tissues. Spectrophotometry was employed to determine total RNA concentration at 260 nm absorbance wavelength, and purity was evaluated by examining the absorbance ratio from 260 nm to 280 nm. Following qualitative and quantitative control of the extracted RNA, the Revert Aid First Strand cDNA Synthesis Kit (Thermo Scientific) was used to reverse transcribe 2 μg of total RNA into cDNA. qRT-PCR in 7500 Fast Real-Time PCR System (Applied Biosystems) and SYBR green Plus reagent kit (Roche) were used to quantify relative concentrations of mRNA. Table 1 showed all the primers used for qRT-PCR. GAPDH was used as the endogenous control and each reaction has three replicates. The comparative $2^{-\Delta\Delta Ct}$ method as described previously was performed to calculate the relative mRNA quantification.[24]

2.14. Analysis of IL-6/STAT3/NF-κB signaling pathway

To analyze the changes of IL-6/STAT3/NF-κB signaling pathway, the western blot analysis was performed. M-PER Mammalian Protein Extraction Reagent (Thermo Scientific) was used to extract total proteins from tumor tissues and then BCA method was used to determine protein concentration. Protein separation was performed on 12% SDS-polyacrylamide gel and separated proteins were then transferred onto PVDF membrane. After blocking in 5% non-fat milk, the membrane was subject to overnight incubation with primary antibodies at 4°C. After washing with PBS-T, the membrane was incubated with horseradish-conjugated secondary

antibodies at room temperature for 1 h. Finally, the membrane was washed and developed with an enhanced chemiluminescence detection system (Millipore, Bedford, MA). Signal intensity was quantified by image analyzer (Image J). The primary antibody used in this study was anti-IL-6 (1:500; Abcam), anti-STAT3 (1:1000; Abcam) and anti-NF-κB (1:800; Abcam). GAPDH was analyzed as internal control with anti-GAPDH antibody (1:1500; Abcam).

2.15. Statistical analysis

Data were expressed as mean ± standard deviation. Using Student-Newman-Keuls Method, student's T-test and ANOVA were employed to analyze experimental results. Kapan-Meier method and log-rank statistical test were used to assess mice survival. $P < 0.05$ was considered statistically significant.

3. Results

3.1. Characteristics of drug-loaded electrospun composite fibers

Well-defined, spherical MSNs of a homogeneous size distribution (average particle size of 121 nm with polydispersity index (PDI) of 0.023) were synthesized, and the SEM, TEM and size distribution of MSN/DOX were shown in the Fig. 1b, c and d, respectively. MSN/DOX were found to load 5.6 mg DOX for 200 mg MSNs, and 120 mg SB was further loaded into the sample of MSN/DOX (200 mg MSN). The results of SEM and TEM for the electrospun composite fibers were shown in Fig. 1e-n, and the fibers of all membranes were uniform with diameters of about 800 nm (Fig. 1 e-i). As demonstrated by the SEM images, co-solvent electrospinning has been proven to be a facile method to fabricate PLLA-MSN composite fibers. Moreover, TEM images illustrated the successful encapsulation of MSN/DOX and MSN/DOX-SB nanoparticles in the fabricated nanofibers (Fig. 1j-n).

3.2. In vitro drug release from composite fibers

Fig. 2 demonstrated the effect of pH on drug release at different conditions. It was found that decrease in pH could generally increase the drug (DOX or IBU) release from all formulations except for that from naked MSNs. The effect of pH was particularly profound when incorporating SB into MSNs. Specifically, at neutral pH,

DOX release from MSN or SB loaded MSN showed similar profile, burst release of approximately 60% at first day and complete release at 4 days (Fig. 2 a). When the pH was reduced, the DOX release from SB loaded MSNs was accelerated compared to its naked counterparts, with more than 90% of DOX released at first day and complete release within two days (Fig. 2 d). When the DOX loaded MSNs were mixed in the PLLA fibers, the DOX release was dramatically reduced probably due to the hydrophobic nature of PLLA, limiting the water sorption and thus slowing the DOX release (compare Fig. 2 a and b). In Fig. 2 b, at neutral pH, DOX release from PLLA fibers exhibited most rapid release (complete release at 40 days), followed by PLLA-(MSN/DOX-SB)-IBU, PLLA-(MSN/DOX-SB), then PLLA-(MSN/DOX) fibers, 28%, 20% and 16% at 40 days and 79%, 69% and 61% at 120 days, respectively. The increase in DOX release from SB loaded PLLA/MSN fibers compared to the naked PLLA/MSN fibers may be due to the high solubility of SB, attracting water penetration and enhancing DOX release. When the pH was reduced, DOX release from PLLA fibers or PLLA/MSN composite fibers with no SB was slightly increased (Fig. 2 e). However, DOX release from PLLA composite fibers with SB loaded MSNs was substantially enhanced, with 36% and 28% at 40 days and 99% and 97% at 120 days, for PLLA-(MSN/DOX-SB)-IBU and PLLA-(MSN/DOX-SB), respectively. Additionally, IBU release was also slightly raised when the pH was reduced, with burst release of 40% at first two days and complete release at 50 days (Fig. 2c and f). The above results have suggested that reducing pH could slightly enhance DOX release from PLLA or PLLA/MSN composite fibers or IBU release from PLLA fibers. However, the addition of SB into MSNs would substantially raise the DOX release, particularly at acidic pH. This may be due to the high solubility of SB and /or the reaction of SB with hydrogen at acidic environment resulting in carbon dioxide (gas) ($NaHCO_3+2H^+ \rightarrow 2Na^+ + H_2O + CO_2$ (↑)), creating channels for DOX diffusion. Besides, addition of IBU into PLLA fibers also increased DOX release. This may be because channels were created during IBU release, allowing more ready water penetration and DOX diffusion from the PLLA fibers.

3.3. Macroscopic and morphological results

As shown in Fig. 3a, we have established the residual HCC model on nude mouse and the developed tumor was resected and implanted with the fibrous scaffolds of different formulations. The wounded area was then sutured to allow further observations of the progression of the residual tumor. The content of lactic acid of the control group gradually increased with time (Fig. 3b), specifically, the content of lactic acid of the second, sixth and tenth weeks was about two times, three times and three times compared with day 0, respectively. These results illustrated that the growth and metabolism of the residual tumor was vigorous with no interference by either the drug or the polymer fibers.

The tumor bearing mice administered with different scaffolds for 3 days, 2, 6 and 10 weeks were observed and the days of survival were presented in Kaplan-Meier's survival analysis curve (Fig. 3c). With PLLA-(MSN/DOX-SB)-IBU fiber treatment, the survival of the tumor bearing mice was significantly longer than the other groups ($P < 0.05$). The % ILS of PLLA-(MSN/DOX-SB)-IBU was 146%, followed by PLLA-(MSN/DOX-SB) (122%), PLLA-MSN/DOX (120%), PLLA-DOX (114%) and PLLA (101%). These results demonstrated that employing IBU to be released for a short term and MSNs to extend DOX release in electrospun PLLA fibers could significantly increase the life span of tumor bearing mice.

H&E images of the tumor tissues after implantation with different materials at different times were shown in Fig. 3d. On the third day after the operation, the tumor tissues in all groups had vigorous growth, there were no obvious necrotic tumor tissues in the control and PLLA group, and the small area of necrotic tumor tissues (indicating decay of tumors) in the drug-loaded groups could be observed. On the second week after the operation, the tumor tissues continued to grow and no obvious necrotic tumor tissues in the control and PLLA group could be seen. In the PLLA-DOX, PLLA-MSN/DOX and PLLA-(MSN/DOX-SB) group, small areas of necrotic tumor tissues could be frequently seen. In the PLLA-(MSN/DOX-SB)-IBU group, the area of necrosis was relatively large compared to all other formulations. On

the sixth week after the operation, there were occasionally necrotic tumor tissues in the control and PLLA group possibly due to lack of nutrition during vigorous growth. Similarly, in the PLLA-(MSN/DOX-SB)-IBU group, the area of necrosis was largest compared to all other groups with DOX. On the tenth week after the operation, the tumor tissues in the PLLA-DOX groups showed a significantly dense growth, comparable with that treated with control and PLLA groups, possibly due to the depletion of loaded drugs. However, the PLLA fibers with MSNs to extend the DOX release have shown continuous presence of frequent small areas of tumor necrosis. It is worth noticing that the PLLA-(MSN/DOX-SB)-IBU group has resulted in large area of necrotic tumor tissues, possibly due to the synergistic effect of addition of IBU.

3.4. Biochemistry markers of apoptosis

The CRP level was relatively high and stable at day 0, the day before the palliative operation in all groups (Fig. 4a). In control and PLLA groups, though the CRP level decreased three days after the operation, which ascribed to the tumor volume reduction surgery, it began to increase gradually from the second week after the operation, indicating development of tumor tissues. In the PLLA-DOX group, the CRP level decreased three days after the operation till the second week, owing to the quick release of DOX whereas the CRP level began to increase from the sixth week till the tenth week, possibly due to depletion of DOX at later time points. In the PLLA-MSN/DOX group, the CRP level decreased at all examined times thanks to the sustained release of DOX. The CRP level decreased more significantly with the PLLA-(MSN/DOX-SB) group, possibly due to the addition of SB to induce the DOX release at acidic environment. The CRP level decreased most dramatically with the PLLA-(MSN/DOX-SB)-IBU group, possibly due to the addition of IBU which inhibited inflammation and further suppressed tumorigenesis.

Activity of caspase 3, apoptosis-related cysteine peptidase, of tumor tissues treated with different groups at different time points was illustrated in Fig. 4d. The caspase-3 activity of the control and PLLA groups increased slowly with time. The

capase-3 activity of the PLLA-DOX group increased rapidly till the second week but slowly till the tenth week possibly due to the initial fast release of DOX and depletion of DOX at later stage. The capase-3 activity of the PLLA-MSN/DOX group increased slowly till the second week but rapidly from sixth to the tenth week possibly due to the slow initial DOX release and more rapid release at later stage due to the extended drug diffusive route from MSN to PLLA and from PLLA to environment. The capase-3 activity of the PLLA-MSN/DOX group exceeded the PLLA-DOX group from the sixth week. The caspase-3 activity of the PLLA-(MSN/DOX-SB) group was higher than that of the PLLA-MSN/DOX group possibly due to the addition of SB which accelerated the DOX release in acidic environment. In PLLA-(MSN/DOX-SB)-IBU group, thanks to the dual-drug loaded system and the pH-responsive property, the caspase-3 activity of PLLA-(MSN/DOX-SB)-IBU group was highest among all the groups at all examined time points.

Fig. 4b demonstrated the immunohistochemical staining of caspase-3 of different groups at the sixth week after operation. In the control and PLLA group, few brown (positive) staining were observed. The positive staining of PLLA fibers with DOX was stronger compared to that treated with no DOX. Among all the groups, the PLLA-(MSN/DOX-SB)-IBU group exhibited strongest positive staining of caspase-3, indicating maximum tumor apoptosis. Quantification of the number of cells with positive stain/mm^2 of demonstrated highest positive cell density for the PLLA-(MSN/DOX-SB)-IBU group, followed by the PLLA-(MSN/DOX-SB), PLLA-MSN/DOX, PLLA-DOX, PLLA and the control group (Fig. 4c).

As shown in Fig. 4e, the relative mRNA expression of Bax in DOX-loaded groups was significantly higher than the control and PLLA group, particularly for the PLLA-(MSN/DOX-SB)-IBU group ($P < 0.0001$). The relative mRNA expression of Bcl-2 in DOX-loaded groups was significantly lower than the control and PLLA group, and the PLLA-(MSN/DOX-SB)-IBU group had the lowest relative mRNA expression of Bcl-2 ($P < 0.0001$) (Fig. 4f). Because of the up-regulation of Bax expression and down-regulation of Bcl-2 expression, the Bax: Bcl-2 ratio from control

to the PLLA-(MSN/DOX-SB)-IBU group demonstrated an increase tendency, indicating increased tumor apoptosis (Fig. 4g).

3.5. Attenuation of IL-6/STAT3/NF-κB signaling pathway in anti-tumor function

It was found that the expression levels of IL-6, STAT3 and NF-κB decreased in DOX-loaded groups compared to the control and PLLA group, and there was no significant difference between the control and PLLA group. However, the expression levels decreased gradually in PLLA-DOX, PLLA-MSN/DOX, PLLA-(MSN/DOX-SB) and PLLA-(MSN/DOX-SB)-IBU group. Notably, the reduction of IL-6 in the PLLA-(MSN/DOX-SB)-IBU group was most significant, possibly due to the incorporation of NSAIDs-IBU which could inhibit the expression of the inflammatory factor-IL-6.

4. Discussion

Low initial burst and long-term release time of DOX from electrospun fibers may be explained by the structures of the composite fibers, and the drug was entrapped in the pores of the MSNs which were further encapsulated in the composite fibers. There were two layers during the process of DOX diffusion from the MSNs into the PLLA fibers and the process of drug diffusion from the PLLA fibers into the release medium. However, the pH responsive feature of SB is a distinctive advantage of the PLLA-(MSN/DOX-SB) and PLLA-(MSN/DOX-SB)-IBU system as it opens up new possibilities for a simple and sensitive cargo delivery. The more rapid delivery of cargo from PLLA-(MSN/DOX-SB) compared to PLLA-(MSN/DOX) may be contributed to the resultant CO_2 gas during reaction of HCO_3^- and H^+, which creates channels inside the fiber and accelerates the drug release. In present study, we successfully synthesized a pH-sensitive dual-drug delivery system with proven anti-tumor capability. Such dual-drug delivery system was found to rapidly release IBU to control the initial inflammation to improve the tumor microenvironment at the early stage, and slowly release the anti-tumor DOX for a long term, leading to improved therapeutic efficacy.

As reported previously, there is close correlation between inflammation and

tumor development, particularly in the liver, for example, HCC almost exclusively arises upon chronic hepatic inflammation.[25] It has been pointed out that NSAIDs could be used in combination with anti-neoplastic agents, such as DOX, as chemosensitizers to improve the treatment responsiveness in cancer patients.[26] Because NSAIDs could resist the multidrug resistance (MDR), which is one of the major reasons for the failure of cancer therapy by inhibiting the activity of P-glycoprotein (P-gp) alone,[26] and a combined chemotherapy of DOX and NSAIDs can reduce the DOX concentration and its side effects without reducing its cytotoxic activity.[27] Besides, treating cancer cells with IBU can significantly up-regulate the glycoprotein surface receptor and tumor suppressor $p75^{NTR}$, which mediates the anti-growth effectiveness.[28] The IBU loaded in our system could be burst released at the early stage, because it was directly incorporated into the electrospun PLLA fibers, which had large surface area to volume ratio. Therefore, it could quickly control the inflammation and play a key role in the anti-tumor activity.

On the other hand, one major difference between many solid tumors and the surrounding normal tissue is the nutrition and metabolic environment.[12] The microenvironment in solid tumor tissues is relatively acidic (pH ≈ 5 to 6.8) compared to that in normal tissues (pH ≈ 7.2 – 7.4).[12] This is the result of lactic acid accumulation caused by anaerobic respiration and/or inability or absence of deficient vascular and lymphatic systems to excrete lactic acid by-products due to high interstitial pressure in tumor tissues.[12] When the $NaHCO_3$ reacts with acid if the acidic solution entered the polymer bulk, CO_2 would be generated, resulting in pores or channels in the polymer, accelerating the DOX release. Thus, in acidic conditions, such as tumor, the drug release rate from the PLLA-(MSN/DOX-SB)-IBU fiber was higher than that from the fibers with no $NaHCO_3$. That is, the drug release could be triggered and raised according to the pH change, leading to a pH responsive drug release with improved therapeutic effect.

It is known that the circulating concentrations of CRP (a nonspecific and acute-phase protein) increases rapidly in response to numerous pathologic and disease

conditions [29] and it is predominantly regulated by IL-6 [30]. In our experiment, the serum concentration of CRP of PLLA-(MSN/DOX-SB)-IBU group was the lowest. It has been reported that IBU may decrease the levels of proinflammatory cytokines such as IL-6 and inflammatory parameters such as CRP due to its anti-inflammatory property,[31] which corresponded well with our results. Caspase-3 plays a significant role in apoptosis due to its ability to cleave cell death substrates and program cellular destruction.[23] And the caspase-3 expression was activated more obviously in the PLLA-(MSN/DOX-SB)-IBU group in our experiment. On the other hand, the up-regulation of Bax, which is a proapoptotic gene, can lead to mitochondrial transmembrane potential loss, cytochrome C release and caspase cascade activation.[32] However, Bcl-2 is the anti-apoptotic molecule regulating the cell death and cell proliferation. Many studies had demonstrated that the Bax: Bcl-2 ratio had increased during the apoptosis,[32] which in line with our qRT-PCR analysis results – the PLLA-(MSN/DOX-SB)-IBU group had the best results in induction of tumor cell apoptosis.

Further, IL-6 is a pluripotent cytokine in inflammatory microenvironment surrounding the tumor, it can promote the malignant progression through regulating many biological processes, including proliferation, survival and invasion.[33] Previous studies suggested that IL-6 was elevated in many cancers, including skin, breast, lung, gastric and liver, etc.[33] Cell survival, proliferation and differentiation are regulated by signal transducers and activators of transcription (STATs), which constitute a family of transcription factors.[34] And the hyperactivation of STAT3 has been shown to promote tumor growth and the suppression of STAT3 signaling has been shown to inhibit cell proliferation, induce apoptosis, stimulate immune responses and suppress angiogenesis in tumor cells.[35] Moreover, the IL-6 can result in downstream target STAT3 activation and induce an oncogenic microenvironment in the liver.[36] NF-κB, which is a crucial transcription factor associated with several human diseases including cancer, can improve cancer cell proliferation, reduce cellular apoptosis and induce more blood flow to enhance the chance of cancer survival.[37] Thus inhibition of

NF-κB activity has potential therapeutic benefit. In one study, the NF-κB pathway conferred resistance to apoptosis through induction of Bcl-2 expression,[38] and inhibition of NF-κB activation in cancer cells resulted in G2/M arrest and cell death.[39] Numerous studies have demonstrated that attenuation of IL-6, STAT3 and NF-κB pathway had a crucial role in suppressing the development of tumor,[33, 36] which corresponded well with our results by western blot analysis. It was also found that IBU could inhibit the expression of CRP and IL-6, and then block the function of IL-6/STAT3/NF-κB signaling pathway. Meanwhile, DOX could prevent NF-κB nuclear translocation and induce the increase of Bax: Bcl-2 ratio. Taken together, these two drugs may play synergistic effect on anti-tumor process. All these findings implied that PLLA-(MSN/DOX-SB)-IBU could significantly inhibit the residual tumor growth after the palliative surgery.

5. Conclusion

We successfully fabricated a novel pH-sensitive electrospun composite PLLA fibrous scaffold, which contained sodium bicarbonate and DOX inside MSNs to achieve long-term pH-sensitive DOX release, and IBU outside MSNs to achieve short-term release. In general, the results of this study demonstrated that the dual-drug loaded system can rapidly release IBU to quickly control the inflammatory factors to improve the tumor microenvironment at the early stage, and sustainably release DOX to prevent the tumor regional recurrence at a relatively later stage. The PLLA-(MSN/DOX-SB)-IBU may inhibit the residual tumor growth after the palliative surgery by the increase of Bax: Bcl-2 ratio and activation of caspase-3 levels, further through the attenuation of IL-6/STAT3/NF-κB signaling pathways. These results have suggested that the proposed strategy in present study may be a promising approach of localized bioresponsive long-term dual drug release which may be translatable to human tumors for prevention of mammary tumor progression. Moreover, the findings in this study have suggested the relation between inflammation and tumorigenesis, which may be employed to control tumor recurrence.

Conflict of Interests

The authors declare that they have no conflict of interests.

Acknowledgements

This work was supported by the National Natural Science Foundation of China (51373112, 81272935 and 81370041), China Scholarship Council (CSC), Jiangsu Provincial Special Program of Medical Science (BL2012004) and the Priority Academic Program Development of Jiangsu Higher Education Institutions.

References

1. Z. Wang, G. Zhang, J. Wu and M. Jia, *Drug. Discov. Ther.*, 2013, 7, 137-143.
2. W. Q. Wang, L. Liu, H. C. Sun, Y. L. Fu, H. X. Xu, Z. T. Chai, Q. B. Zhang, L. Q. Kong, X. D. Zhu, L. Lu, Z. G. Ren and Z. Y. Tang, *J. Hematol. Oncol.*, 2012, 5, 69.
3. A. Forner, J. M. Llovet and J. Bruix, *Lancet.*, 2012, 379, 1245-1255.
4. I. Garcia-Alonso, T. Palomares, A. Alonso, M. Echenique-Elizondo, J. Carames, B. Castro and J. Méndez, *J. Surg. Res.*, 2008, 148, 185-190.
5. E. C. Lai, S. T. Fan, C. M. Lo, K. M. Chu, C. L. Liu and J. Wong, *Ann. Surg.*, 1995, 221, 291-298.
6. P. C. Kwok, T. W. Lam, P. W. Lam, K. W. Tang, S. C. Chan, J. S. Hwang, M. T. Cheung, D. L. Tang, T. K. Chung, N. H. Chia, W. K. Wong, M. K. Chan, H. Y. Lo and W. M. Lam, *J. Gastroenterol. Hepatol.*, 2003, 18, 450-455.
7. E. C. Lai, C. M. Lo, S. T. Fan, C. L. Liu and J. Wong, *Arch Surg.*, 1998, 133, 183-188.
8. I. P. Witz and O. Levy-Nissenbau, *Cancer. Lett.*, 2006, 242, 1-10.
9. K. M. Sakthivel and C. Guruvayoorappan, *Asian. Pac. J. Cancer. Prev.*, 2013, 14, 3909-3919.
10. Y. Oka, Y. Akagi, T. Kinugasa, N. Ishibashi, N. Iwakuma, I. Shiratsuchi and K. Shirouzu, *Anticancer. Res.*, 2013, 33, 2887-2894.
11. C. K. Hee, J. S. Dines, D. M. Dines, C. M. Roden, L. A. Wisner-Lynch, A. S. Turner, K. C. McGilvray, A. S. Lyons, C. M. Puttlitz and B. G. Santoni, *Am. J. Sports. Med.*, 2011, 39, 1630-1639.
12. I.F. Tannock and D. Rotin, *Cancer. Res.*, 1989, 49, 4373-4384.
13. Z. Yuan, J. Zhao, Y. Chen, Z. Yang, W. Cui and Q. Zheng, *Mediators. Inflamm.*, 2014, 2014, 11.
14. Z. Hou, X. Li, C. Li, Y. Dai, P. Ma, X. Zhang, X. Kang, Z. Cheng and J. Lin, *Langmuir.*, 2013, 29, 9473-9482.
15. C. Hu, S. Liu, Y. Zhang, B. Li, H. Yang, C. Fan and W. Cui, *Acta Biomater.*, 2013,

9, 7381-7388.

16. C. Hu and W. Cui, *Adv. Healthc. Mater.*, 2012, 1, 809-814.
17. R. Izumi, K. Shimizu, T. Iyobe, T. Ii, M. Yagi, O. Matsui, A. Nonomura and I. Miyazaki, *Hepatology.*, 1994, 20, 295-301.
18. M. Manzano, V. Aina, C. O. Areán, F. Balas, V. Cauda, M. Colilla, M. R. Delgado and M. Vallet-Regi, *Chem. Eng. J.*, 2008, 137, 30-37.
19. K. X. Qiu, C. L. He, W. Feng, W. Z. Wang, X. J. Zhou, Z. Q. Yin, L. Chen, H. S. Wang and X. M. Mo, *J. Mater. Chem. B.*, 2013, 1, 4601-4611.
20. S. Saraswati, S. S. Agrawal and A. A. Alhaider, *Chem. Biol. Interact.*, 2013, 206, 153-165.
21. A. Mantovani, C. Garlanda, A. Doni and B. Bottazzi, *J. Clin. Immunol.*, 2008, 28, 1-13.
22. V. Bronte, *Immunol. Cell. Biol.*, 2014, 92, 647-649.
23. B. T. Hyman and J. Yuan, *Nat. Rev. Neurosci.*, 2012, 13, 395-406.
24. K. J. Livak and T. D. Schmittgen, *Methods.*, 2001, 25, 402-408.
25. H. B. El-Serag and K. L. Rudolph, *Gastroenterology.*, 2007, 132, 2557-2576.
26. A. Angelini, M. Iezzi, C. Di Febbo, C. Di Ilio, F. Cuccurullo and E. Porreca, *Oncol. Rep.*, 2008, 20, 731-735.
27. P. Andrews, X. Zhao, J. Allen, F. Li and M. Chang, *Cancer. Chemother. Pharmacol.*, 2008, 61, 203-214.
28. F. Khwaja, J. Allen, J. Lynch, P. Andrews and D. Djakiew, *Cancer. Res.*, 2004, 64, 6207-6213.
29. K. H. Allin and B. G. Nordestgaard, *Crit. Rev. Clin. Lab. Sci.*, 2011, 48, 155-170.
30. P. C. Heinrich, J. V. Castell and T. Andus, *Biochem. J.*, 1990, 265, 621-636.
31. M. M. Arons, A. P. Wheeler, G. R. Bernard, B. W. Christman, J. A. Russell, R. Schein, W. R. Summer, K. P. Steinberg, W. Fulkerson, P. Wright, W. D. Dupont and B. B. Swindell, *Crit. Care. Med.*, 1999, 27, 699-707.
32. T. Bowman, R. Garcia, J. Turkson and R. Jove, *Oncogene.*, 2000, 19, 2474-2488.
33. Y. Guo, F. Xu, T. Lu, Z. Duan and Z. Zhang, *Cancer. Treat. Rev.*, 2012, 38,

904-910.

34. P. Deng, C. Wang, L. Chen, C. Wang, Y. Du, X. Yan, M. Chen, G. Yang and G. He, *Biol. Pharm. Bull.*, 2013, 36, 1540-1548.
35. J. Bollrath, T. J. Phesse, V. A. von Burstin, T. Putoczki, M. Bennecke, T. Bateman, T. Nebelsiek, T. Lundgren-May, O. Canli, S. Schwitalla, V. Matthews, R. M. Schmid, T. Kirchner, M. C. Arkan, M. Ernst and F. R. Greten, *Cancer cell.*, 2009, 15, 91-102.
36. G. He, G. Y. Yu, V. Temkin, H. Ogata, C. Kuntzen, T. Sakurai, W. Sieghart, M. Peck-Radosavljevic, H. L. Leffert and M. Karin, *Cancer cell.*, 2010, 17, 286-297.
37. L. Xu and W. A. Russu, *Bioorg. Med. Chem.*, 2013, 21, 540-546.
38. S. D. Catz and J. L. Johnson, *Oncogene.*, 2001, 20, 7342-7351.
39. S. Savion, G. Oserov, H. Orenstein, A. Torchinsky, A. Fein and V. Toder, *TToxicol. In. Vitro.*, 2013, 27, 804-811.

Figure Caption

Fig. 1. (a) An illustration of drug-loaded electrospun fibers implanted into hepatocellular carcinoma lesions. (b) SEM image of MSN/DOX, (c) TEM image of MSN/DOX and (d) size distribution of MSN/DOX. SEM (e-i) and TEM (j-n) images of PLLA (e and j), PLLA-DOX (f and k), PLLA-MSN/DOX (g and l), PLLA-(MSN/DOX-SB) (h and m) and PLLA-(MSN/DOX-SB)-IBU (i and n) fibers.

Fig. 2. DOX and IBU release from MSN/DOX, MSN/DOX-SB, PLLA-DOX, PLLA-MSN/DOX, PLLA-(MSN/DOX-SB) and PLLA-(MSN/DOX-SB)-IBU electrospun fibers in pH7.4 and pH 5.0 PBS at 37°C.

Fig. 3. (a) Images showing resection procedure. The yellow circles represent (i) tumor formation in nude mice; (ii) segmental resection of the tumor; (iii) implantation of fibrous scaffold into the residual tumor of nude mice; (iv) suture of the wounded area. (b) The lactic acid content of tumor tissue. (c) Kaplan-Meier's survival analysis curve. To determine the mean survival time (MST) and percentage increased life span (% ILS), animals were allowed to progress to a natural death. (d) Histopathological analysis of mice with liver residual tumor. The black arrows in the Fig.s represent the necrosis of tumor tissues.

Fig. 4. (a) The CRP concentration, (b) the immunohistochemical staining of caspase-3 at the sixth week after operation (the black arrows represent the positive staining), (c) the caspase-3 positive cells (103) per mm2 (** $P < 0.01$ compared with control group), (d) the caspase-3 activity (e) qRT-PCR analysis of Bax expression, (f) Bcl-2 expression, and (g) Bax: Bcl-2 ratio at the sixth week after operation of control, PLLA, PLLA-DOX, PLLA-MSN/DOX, PLLA-(MSN/DOX-SB) and PLLA-(MSN/DOX-SB)-IBU group. Data were presented as mean values ± SD (n=5). ** $P < 0.0001$ represents significant difference compared to control group.

Fig. 5. Western blot analysis of IL-6/STAT3/NF-κB signaling pathway on the sixth week after operation. (a) The protein levels of IL-6, STAT3 and NF-κB. (b-d) The analysis of the signal intensity of IL-6, STAT3, and NF-κB, respectively of control, PLLA, PLLA-DOX, PLLA-MSN/DOX, PLLA-(MSN/DOX-SB) and PLLA-(MSN/DOX-SB)-IBU group.**$P < 0.01$ compared to control group.

Fig. 6. The schematic diagram of suggested synergistic effect of drugs on anti-tumor process. IBU inhibits the expression of CRP and IL-6, and then block the function of IL-6/STAT3/NF-κB signaling pathway. Meanwhile, DOX prevents NF-κB nuclear translocation and induce the increase of Bax: Bcl-2 ratio, leading to the release of cytochrome c from the mitochondria. And the cytochrome c activates Caspase pathway molecules, finally resulting in to cell apoptosis.

Figures

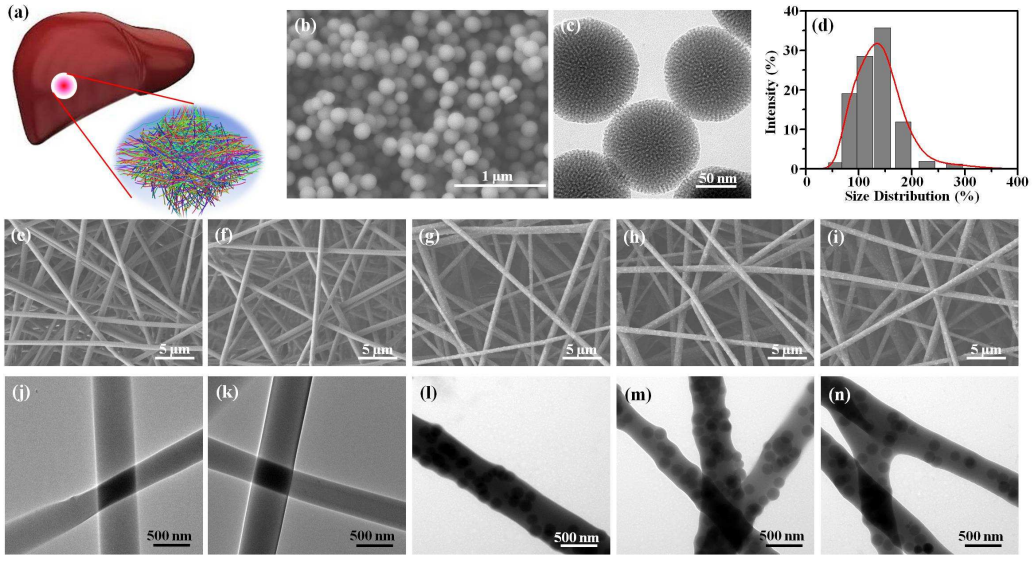

Fig. 1. (a) An illustration of drug-loaded electrospun fibers implanted into hepatocellular carcinoma lesions. (b) SEM image of MSN/DOX, (c) TEM image of MSN/DOX and (d) size distribution of MSN/DOX. SEM (e-i) and TEM (j-n) images of PLLA (e and j), PLLA-DOX (f and k), PLLA-MSN/DOX (g and l), PLLA-(MSN/DOX-SB) (h and m) and PLLA-(MSN/DOX-SB)-IBU (i and n) fibers.

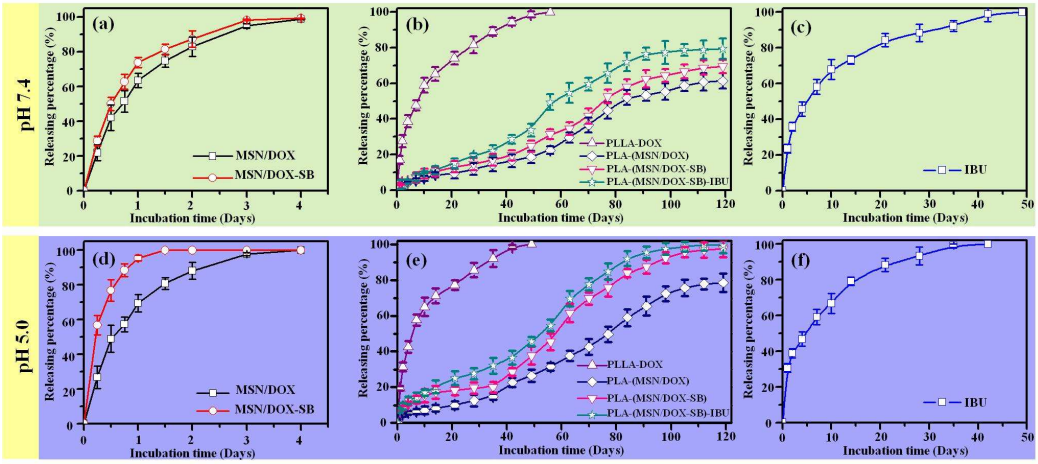

Fig. 2. DOX and IBU release from MSN/DOX, MSN/DOX-SB, PLLA-DOX, PLLA-MSN/DOX, PLLA-(MSN/DOX-SB) and PLLA-(MSN/DOX-SB)-IBU electrospun fibers in pH7.4 and pH 5.0 PBS at 37°C

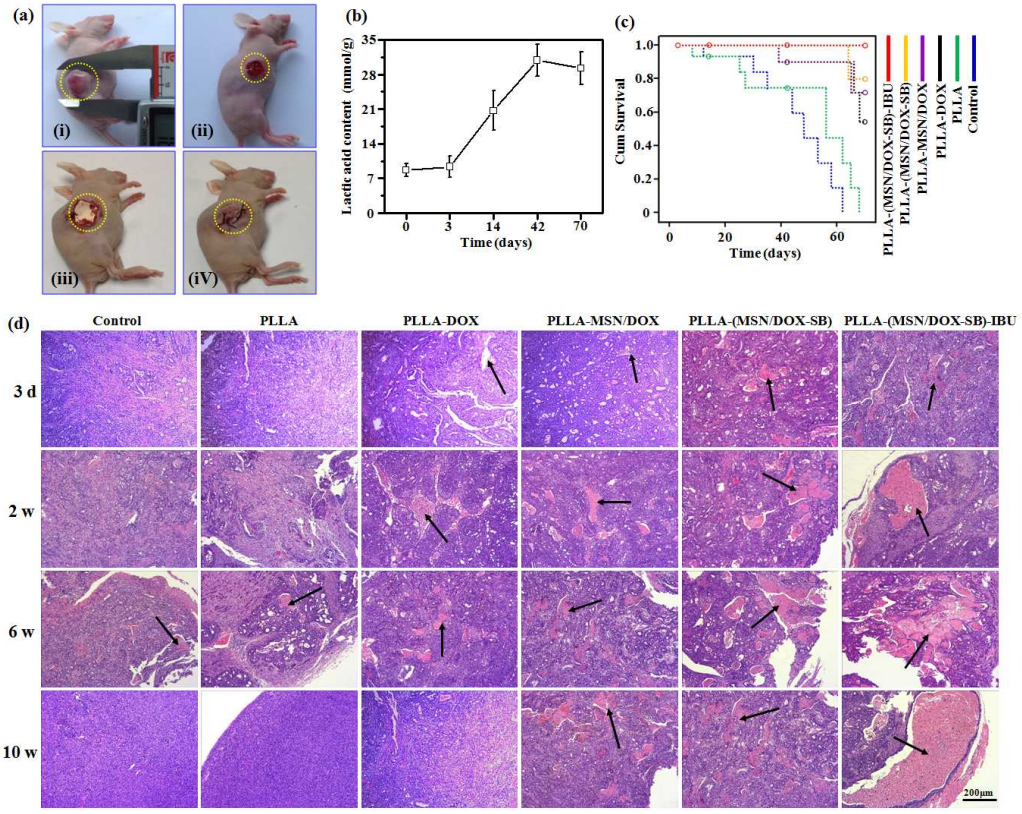

Fig. 3. (a) Images showing resection procedure. The yellow circles represent (i) tumor formation in nude mice; (ii) segmental resection of the tumor; (iii) implantation of fibrous scaffold into the residual tumor of nude mice; (iv) suture of the wounded area. (b) The lactic acid content of tumor tissue. (c) Kaplan-Meier's survival analysis curve. To determine the mean survival time (MST) and percentage increased life span (% ILS), animals were allowed to progress to a natural death. (d) Histopathological analysis of mice with liver residual tumor. The black arrows in the figures represent the necrosis of tumor tissues.

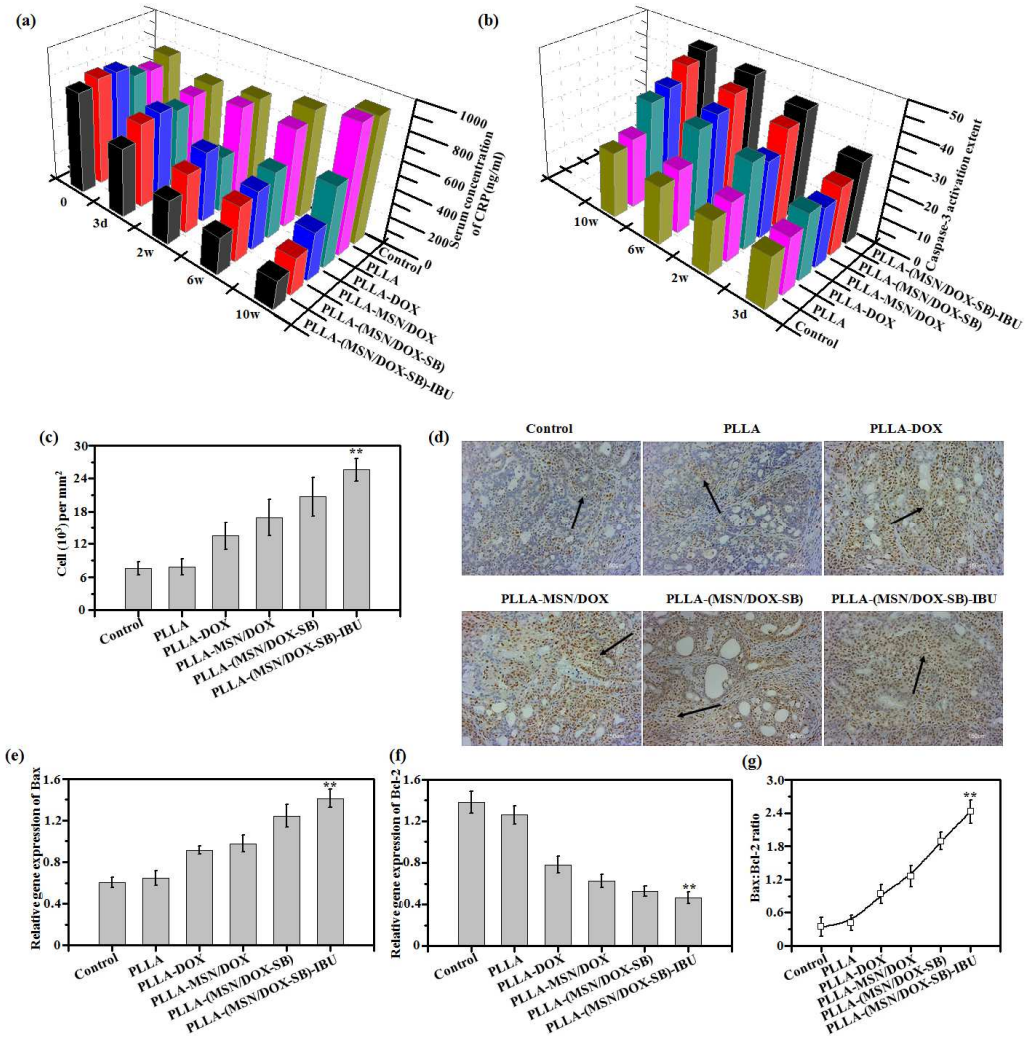

Fig. 4. (a) The CRP concentration, (b) the immunohistochemical staining of caspase-3 at the sixth week after operation (the black arrows represent the positive staining), (c) the caspase-3 positive cells (10^3) per mm^2 (** $P < 0.01$ compared with control group), (d) the caspase-3 activity (e) qRT-PCR analysis of Bax expression, (f) Bcl-2 expression, and (g) Bax: Bcl-2 ratio at the sixth week after operation of control, PLLA, PLLA-DOX, PLLA-MSN/DOX, PLLA-(MSN/DOX-SB) and PLLA-(MSN/DOX-SB)-IBU group. Data were presented as mean values ± SD (n=5). ** $P < 0.0001$ represents significant difference compared to control group.

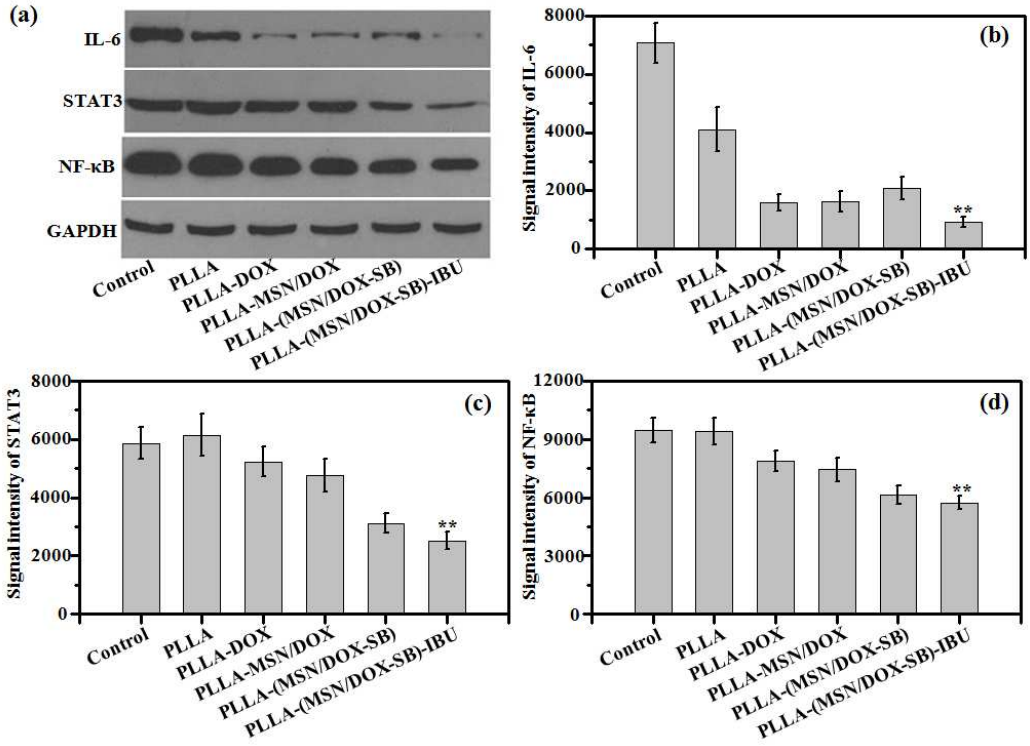

Fig. 5. Western blot analysis of IL-6/STAT3/NF-κB signaling pathway on the sixth week after operation. (a) The protein levels of IL-6, STAT3 and NF-κB. (b-d) The analysis of the signal intensity of IL-6, STAT3, and NF-κB, respectively of control, PLLA, PLLA-DOX, PLLA-MSN/DOX, PLLA-(MSN/DOX-SB) and PLLA-(MSN/DOX-SB)-IBU group.**$P < 0.01$ compared to control group.

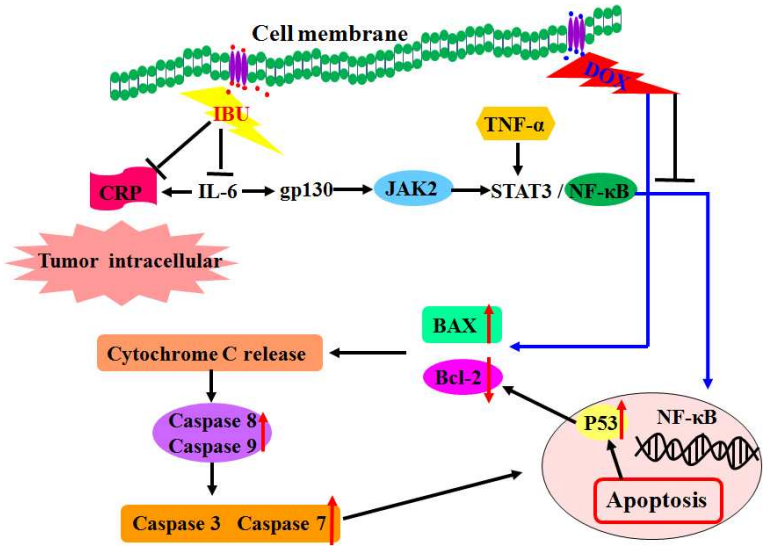

Fig. 6. The schematic diagram of suggested synergistic effect of drugs on anti-tumor process. IBU inhibits the expression of CRP and IL-6, and then block the function of IL-6/STAT3/NF-κB signaling pathway. Meanwhile, DOX prevents NF-κB nuclear translocation and induce the increase of Bax: Bcl-2 ratio, leading to the release of cytochrome c from the mitochondria. And the cytochrome c activates Caspase pathway molecules, finally resulting in to cell apoptosis.

Table 1 Primer sequences of different genes

	Sense	Antisense
Bcl-2	5' AGACCGAAGTCCGCAGAACC 3'	5' GAGACCACACTGCCCTGTTG 3'
Bax	5' AGCTGAGCGAGTGTCTCAAG 3'	5' TGTCCAGCCCATGATGGTTC 3'
GAPDH	5' CACCCACTCCTCCACCTTTG 3'	5' CCACCACCCTGTTGCTGTAG 3'

Graphical Abstract

A novel pH-sensitive electrospun composite PLLA fibrous scaffold was designed for achieving long-term pH-sensitive doxorubicin release and short-term ibuprofen release, which may inhibit the residual tumor growth after the palliative surgery by the increase of Bax: Bcl-2 ratio and activation of caspase-3 levels, further through the attenuation of IL-6/STAT3/NF-κB signaling pathways.